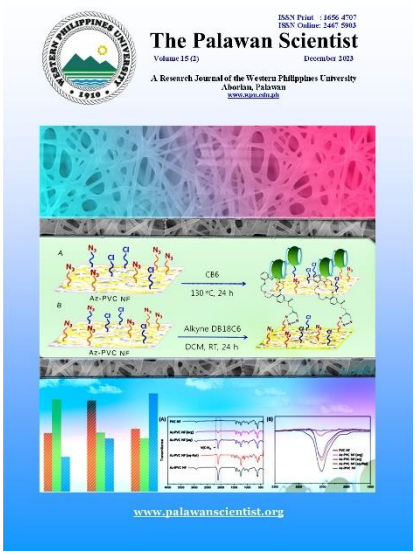

ISSN: 1656-4707
E-ISSN: 2467-5903
Homepage: www.palawanscientist.org

Numerical modeling of the drying behavior of Adlai (*Coix lacryma-jobi* L.) grain

Alvin M. Ante[1*], Arnold R. Elepaño[2], Kevin F. Yaptenco[2] and Delfin C. Suministrado[3]

[1]*Department of Agricultural and Biosystems Engineering, College of Engineering, Dr. Emilio B. Espinosa Sr. Memorial State College of Agriculture and Technology, Mandaon, Masbate, Philippines*
[2]*Agricultural, Food and Bio-process Engineering Division, Institute of Agricultural and Biosystems Engineering, College of Engineering and Agro-Industrial Technology, University of the Philippines Los Baños, Laguna, Philippines*
[3]*Agribiosystems Machinery and Power Engineering Division, Institute of Agricultural and Biosystems Engineering, College of Engineering and Agro-Industrial Technology, University of the Philippines Los Baños, Laguna, Philippines*
**Correspondence: amante@up.edu.ph or antealvin@gmail.com*

Received: 31 May 2023 || Revised: 17 Oct. 2023 || Accepted: 28 Nov. 2023
https://doi.org/10.69721/TPS.J.2023.15.2.06

How to cite:
Ante AM, Elepaño AR, Yaptenco KF and Suministrado DC. 2023. Numerical modeling of the drying behavior of Adlai (*Coix lacryma-jobi* L.) grain. The Palawan Scientist, 15(2): 55-68. https://doi.org/10.69721/TPS.J.2023.15.2.06

ABSTRACT

The study aimed to develop computational fluid dynamics (CFD) models for simulating the drying performance of Adlai grain during convective drying with an air temperature range of 30°C to 60°C at around 10% to 80% relative humidity (RH). Before CFD modeling, the calculation of selected thermophysical properties of Adlai through mathematical modeling of its food constituents and thin-layer drying experiments were conducted. The simulation of heat and mass (moisture) transfer and visualization of moisture and temperature gradients in Adlai grain during drying were carried out using Analysis Systems (Ansys) Student 2020 R2 software package, specifically the Fluent solver. Results showed that the CFD models exhibited good agreement with the actual drying performance of Adlai. The models were validated using three statistical parameters: coefficient of determination (R^2), standard error (S), and percent mean deviation modulus (P%). The R^2 values ranged from 0.94-0.98; the S values ranged from 0.0018-0.0066; and the P% values ranged from 6.5%-8.68%. Overall, the models were deemed acceptable in estimating the moisture content of Adlai due to high R^2 values, low S values, and P% values of less than 10%. The results validate the use of CFD as a reliable method for predicting the drying performance of Adlai, which contributes to the optimization of the drying process, the improved designing of drying systems, and the enhancement of product quality.

Keywords: grain drying, hot air, multiphysics, simulation

INTRODUCTION

The Bureau of Agricultural Research (BAR) has initiated research and development activities on Adlai (*Coix lacryma-jobi*) since 2011. It saw the highly nutritious Adlai grain or "Job's tears" as a potential alternative to rice as a staple food. Approximately, the Adlai grain contains the following: 9.9-10.8% water; 13.6-19.1% protein; 5.7-6.1% fat; 58.5–62.7% carbohydrate; 8.4% fiber and 2.2-2.6% ash (Aradilla 2018). Compared to rice and corn, Adlai has higher food energy, carbohydrates, protein, fat, and dietary fiber. It also has the following minerals: calcium, phosphorus, iron, niacin, thiamine, and riboflavin (Peñaflor et al. 2014). Three of its varieties are endemic in the Philippines – "guilian", "ginampay", and "pulot". Research and other related activities have also been done by other agencies such as the Department of Agriculture (DA) and the Philippine Center for Post-Harvest Mechanization and

Development (PhilMech) to study and enhance Adlai's production, post-harvest operations, and commercialization.

Currently, Adlai is grown and consumed in areas such as Zamboanga del Sur, Isabela, Batangas, Caraga Region, and the Bicol Region. The production of Adlai follows the same traditional method for rice production. The "ginampay" variety of Adlai could produce a yield of 3.4 tons/ha, which is just slightly lower than the average rice yield of 3.87 tons/ha. The traditional processing of Adlai after harvesting involves drying and milling. Sun-drying of threshed grains occurs two days before milling (Aradilla 2018). Unhulled Adlai grains sell for around PHP 200.00 per kg, while milled grains go for around PHP 300.00 to PHP 500.00 per kg.

There are studies on the processing of Adlai into several products, such as ice cream (Khongjeamsiri 2007), yogurt (Keeratibunharn and Krasaekoopt 2013), and saltine crackers (Andoy et al. 2019). However, some of its post-harvest qualities, such as its drying characteristics and equilibrium moisture content (EMC), remain unknown. Drying is one of the most fundamental and indispensable unit operations in grain processing. It is performed to reduce the moisture content level in food and other biological materials with the aim to prolong its shelf life, reducing the probability of fungi development, and facilitating further processing to obtain a finished product available for consumption, utilization, and other purposes. For cereal grains like Adlai, proper drying must be performed to improve grain quality and storage time. Convective and radiation drying methods are the two general types of drying methods used for grains. These methods are embodied in the commonly used and preferred drying operations in the Philippines: sun-drying and convective drying. The latter is a complex process that involves simultaneous heat and mass (moisture) transfer, change in physical properties, and shrinkage of biological material (Kumar et al. 2012). Convection drying is performed by supplying heated air to a batch of grains via a blower or fan. Moisture removal results from the vaporization of moisture before being taken away by the air stream.

Convection drying of agricultural products, such as grains, is both energy and time-consuming. The food processing industry needs to obtain high-quality dry products utilizing only the lowest possible amount of energy input, including labor, and the shortest drying time. With the powerful computing capabilities of programs like Ansys Fluent, Ansys CFX, COMSOL Multiphysics, etc. numerical modeling of the drying phenomena in grains became achievable. This is done by computational fluid dynamics (CFD) simulation employed by such programs to aid engineers and scientists in solving multiphysics problems involving mass, momentum, and energy transfer. In studying the drying kinetics of agricultural and biological products, CFD has become a common practice among food engineers and technologists due to its energy, time, and cost-saving benefits in contrast to laborious experimentation. However, actual experiments are still helpful in validating the models. For grains like Adlai, a well-developed CFD model can provide a more accurate and efficient description of its drying behavior.

The study aimed to develop CFD models for simulating the drying performance of Adlai grain by numerical modeling of the heat and mass (moisture) transfer in the kernel during convective drying. Specifically, the study aimed to calculate the selected thermophysical properties of Adlai grain needed for CFD simulation; to perform a thin-layer drying experiment of Adlai grain, to perform CFD modeling using multiphysics software, and to validate the CFD-generated drying curves of Adlai grain with the experimental results. Through numerical simulations, predicting the drying behavior of Adlai under various drying conditions would be possible and would contribute to optimizing further drying systems, equipment, and practices for Adlai.

METHODS

Thermophysical Properties of Adlai

Values for selected thermophysical properties of Adlai were calculated using mathematical models developed by Choi and Okos (1986) that used the proximate composition or fraction of food constituents of the product (Ibarz and Barbosa-Canovas 2014). The models or equations used in the study were expressed as a function of temperature in the range of -40°C to 150°C. These equations are presented in Table 1.

Properties of the Drying Air

The properties of the drying air used in the convection drying of Adlai are necessary in developing the CFD models. They were used in the material properties panel of the fluid cell zone of the models. Table 2 presents the values for the different air properties used in the CFD simulations.

Thin-Layer Drying Experiment

The initial moisture content of sample Adlai grains in MC d.b. (moisture content dry basis) was calculated using the conventional air oven method, following the recommended procedures from the American Society of Agricultural Engineers (ASAE) Standards for moisture measurement of unground grain and seeds. There is no recommended oven temperature, sample size, and heating period for Adlai yet. However, for the purpose of the study, the maximum allowable oven temperature of 130°C was used along with the standard sample size of 10 g and

heating period of 18 h. This method was also adopted by Kim et al. (2016) in thin-layer drying of sorghum. The study used the "guilian" variety of Adlai due to its availability and cultivation for human consumption.

The grain samples were stored at 10°C in cold storage for seven days and were subjected to room temperature 24 h prior to the commencement of the thin-layer drying experiment. A tunnel dryer consisting of a blower, ducts, a heating element, and a temperature controller was used to supply heated drying air to the single layer of Adlai grains resting on a perforated stainless-steel drying tray. The mass of the grains used was around 35 g per replication. The dryer's schematic design is shown in Figure 1.

Table 1. Mathematical models used to estimate the thermophysical properties of Adlai (Ibarz and Barbosa-Canovas 2014; Carson et al. 2016).

Property	Food Component	Property Model (*t = temperature in °C*)	Equation/s
Thermal conductivity (k), W/m-K	Protein	k = 1.7881E-01 + 1.1958E-03*t* - 2.7178E-06*t*^{2}	$k_I = \frac{\Sigma(k_i v_i)}{\Sigma v_i}$ $k_{III} = \frac{(3v_a-1)k_a+[3(1-v_a)-1]k_I+\sqrt{\{(3v_a-1)k_a+[3(1-v_a)-1]k_I\}^2+8k_Ik_a}}{4}$ where: k_I = thermal conductivity from Parallel Model, W/m-K k_{III} = thermal conductivity from Effective Medium Theory model, W/m-K v_a = volume fraction of air v_i = volume fraction of food constituent k_a = thermal conductivity of air, W/m-K
	Fat	k = 1.8071E-01 - 2.7604E-04*t* - 1.7749E-07*t*^{2}	
	Carbohydrate	k = 2.0141E-01 + 1.3784E-03*t* - 4.3312E-06*t*^{2}	
	Fiber	k = 1.8331E-01 + 1.2497E-03*t* - 3.1683E-06*t*^{2}	
	Ash	k = 3.2962E-01 + 1.4011E-03*t* - 2.9069E-06*t*^{2}	
Density (ρ), kg/m^3	Protein	ρ = 1.3299E-03 - 5.1840E-01*t*	$\rho = \frac{(1-\varepsilon)}{\Sigma(x_i/\rho_i)}$ where: ρ = true density, kg/m^3 ε = porosity x_i = mass fraction of food constituent ρ $_i$ = density of food constituent, kg/m^3
	Fat	ρ = 9.2559E02 - 4.1757E-01*t*	
	Carbohydrate	ρ = 1.5991E03 - 3.1046E-01*t*	
	Fiber	ρ = 1.3115E03 - 3.6589E-01*t*	
	Ash	ρ = 2.42385E03 - 2.8063E-01*t*	
Specific heat (C_p), kJ/kg-K	Protein	c_p = 2.0082 + 1.2089 E-03*t* – 1.3129 E-06*t*^{2}	$c_u = \Sigma(c_i x_i)$ where: c_u = specific heat, kJ/kg-K c_i = specific heat of food constituent, kJ/kg-K x_i = mass fraction of food constituent
	Fat	c_p =1.9842 + 1.4733E–03*t* – 4.8008E-06*t*^{2}	
	Carbohydrate	c_p =1.5488 + 1.9625E-03*t* – 5.9399 E-06*t* ^{2}	
	Fiber	c_p = 1.8459 + 1.8306E-03*t* – 4.6509E-06*t* ^{2}	
	Ash	c_p = 1.0926 + 1.8896 E-03*t* – 3.6817 E-06*t* ^{2}	
Water	Thermal conductivity	k_w = 5.7109 E-01 + 1.7625E-03*t* – 6.7036E-06*t* ^{2}	
	Density	ρ_w = 9.9718E02 + 3.1439E-03*t* – 3.7574E-03*t* ^{2}	
	Specific heat (for temperature range of 0 to 150 °C)	c_w = 4.1289 – 9.0864 E-05*t* + 5.4731E-06*t* ^{2}	

The Adlai grain samples were subjected to forced heated air drying at three drying air temperatures: 30°C (ambient), 45°C, and 60°C. These temperature values were selected for the study since a drying air temperature of 30°C represents the average ambient air temperature; 45°C drying air was used relative to maintaining seed viability; and 60°C drying air was used for commercial drying. A constant air velocity of around 1 m/s was used during the experiment. The drying air temperature was maintained during drying via a temperature controller (Elitech STC-1000 Temperature Controller), while the velocity of the drying air was monitored via an anemometer (PEAKMETER® Digital Anemometer PM6252A).

Table 2. Air properties used at various drying air temperatures.

Property	Drying Air Temperature (ºC)			References
	30	45	60	
Density, kg/m^3	1.164	1.109	1.059	Cengel and Cimbala 2014
Specific heat, J/kg-K	1007	1007	1007	
Thermal conductivity, W/m-K	0.02588	0.02699	0.02808	
Dynamic viscosity, kg/m-s	1.87 x 10^{-05}	1.94 x 10^{-05}	2.01 x 10^{-05}	
Diffusion coefficient of water into air, kg/m-s	3.118 x 10^{-05}	3.299 x 10^{-05}	3.469 x 10^{-05}	The Engineering ToolBox 2018

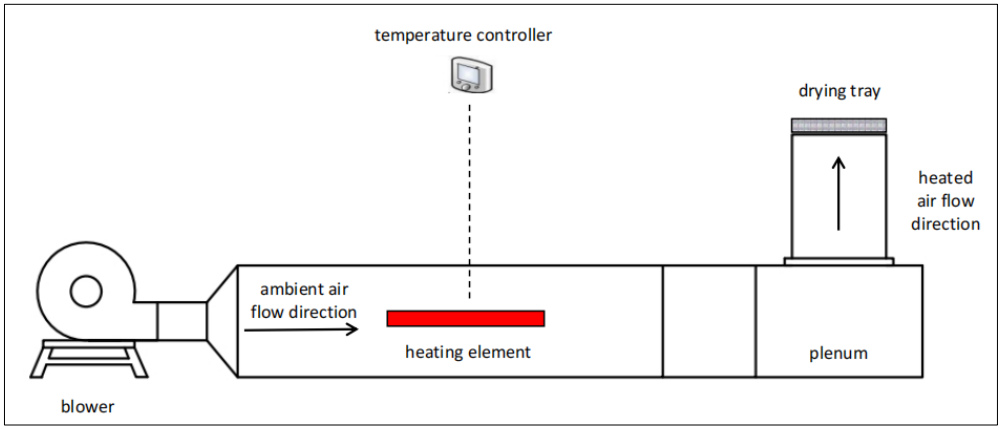

Figure 1. Schematic of the dryer used for thin-layer drying of Adlai.

The relative humidity (RH) during drying was monitored using a digital thermohygrometer (Senze Instruments Digital Hygro Thermometer TH-D-TH06OH). The change in mass of the grains was recorded manually at intervals recommended by ASAE standards: every 5 seconds during the first 5 min, every 1 min during the next hour, and every 15 min after that. An electronic balance was used for calculating the change in mass of the grain samples (Shenzhen Big Dipper Scale Co., Ltd., BDS-PN PN602A). Subsequently, the drying curve was generated from the experiment. Drying was performed until equilibrium was reached between the Adlai grains and the drying air. The experiment was conducted in triplicate per treatment of drying air temperature.

Fick's second law of diffusion was also used to describe the drying phenomenon since thin-layer drying occurred in the falling rate period, and diffusion of moisture inside the kernel is the resistance factor governing the process. The simplified diffusion model is based on the solution of Henderson's moisture diffusion law (Kim et al. 2016). The model is expressed as:

$$MR=Aexp(-kt) \quad (1)$$

where A and k are model constants. The drying constant, k, is expressed as per unit time. The time duration of drying is represented by t, usually in hours or minutes.

The average effective diffusivity (D_e) values of Adlai grain moisture at different drying air temperatures were calculated from the experimental drying curves and were used in the CFD simulations. It was assumed to be constant during the drying process. The effect of drying air temperature on effective diffusivity was represented through an exponential model (Peleg et al. 2012) expressed as

$$D_e = D_o exp(cT_a) \quad (2)$$

where D_e is the effective diffusivity (m^2/s), D_o is a diffusivity at infinite high temperature, c is a constant (1/K), and T_a is the drying air temperature (K).

Computational Fluid Dynamics (CFD) Drying Simulation of Single Adlai Kernel

Thin-layer drying can be considered as grain being immersed in fluid (Prakash and Pan 2011); hence, its mechanism can be described by single kernel drying and its governing equations. This was reflected in the study of Chen et al. (2023) on the heat and mass transfer modeling of a single-particle peanut, wherein the numerical model was validated by a thin-layer drying experiment using hot air. The following steps were adopted to create the CFD drying models for a single Adlai kernel: (1) generating the model geometry, (2) mesh/grid generation, (3) setting up the Fluent solver, (4) numerical solution with Fluent, and (5) post-processing. The multiphysics software used for the study was Ansys Student 2020 R2, which is a free academic version of the Ansys software package. Computational fluid dynamics simulations were explicitly conducted using the Fluent solver of Ansys Student.

The 3D teardrop geometry representing the Adlai or "Job's tears" kernel was made using AutoCAD 2016 software by Autodesk®. The average major and minor axes of the kernel were calculated from the measurement of 20 Adlai grain samples using a Vernier caliper (1/128 in). The 3D Adlai model was further enhanced when imported into DesignModeler, an object-generating component of Fluent, as shown in Figure 2. The flow field for the drying air was added as an enclosure surrounding the kernel geometry. The mesh of the CFD simulations resulted in 212,436 elements and 43,710 nodes. Since the study used the Ansys Student version only, the mesh was refined to a level where further refinement did not enhance the results of the numerical solution. Unstructured tetrahedral elements were used as recommended for 3D meshing. Inflation was used on the walls of the kernel for improved gradient calculation. Quadrilateral cells were used for inflation along the surface of the kernel. The mesh of the kernel geometry is presented in Figure 3.

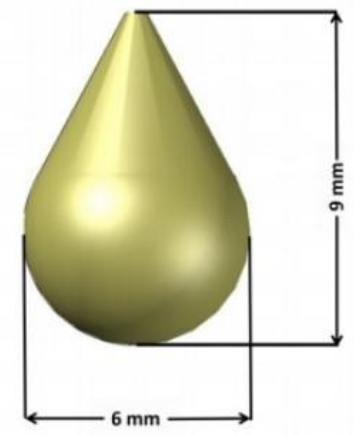

Figure 2. The 3D geometry of single Adlai grain.

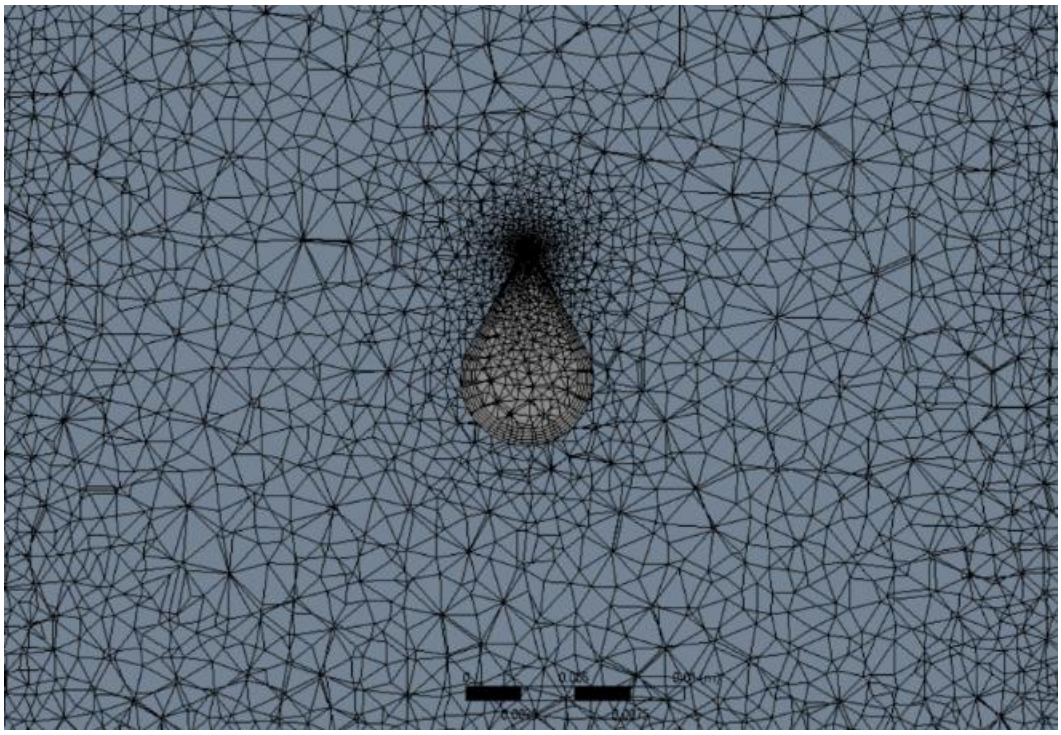

Figure 3. Unstructured mesh (cross-section) of the computational fluid dynamics (CFD) model for convective drying of Adlai grain.

Before proceeding with the development of the CFD simulations using Fluent, specific assumptions about the model were established based on the earlier works of other researchers in the field of CFD and its applications in drying biological products. The following were the governing assumptions adopted for the CFD models in the study: (1) no variation in shape and size of the kernel during drying, (2) the kernel is considered homogeneous, (3) uniform moisture distribution, (4) constant effective diffusivity and convective mass transfer coefficient during diffusion, (5) diffusion is the only transport mechanism of moisture inside the kernel, (6) moisture transfer to the drying air only occurs at the kernel surface, and (7) no volumetric heat generation within the kernel (ElGamal et al. 2014; Chilka and Ranade 2018). The geometry used in the simulations was considered a homogeneous lumped model of the Adlai grain. The thermophysical properties of the grain were applied to the lumped model's entirety because there is no available information from literature on the specific values for the endosperm, bran, and hull of Adlai. Furthermore, grains, in general, are practically dried as a whole with the kernel, bran, and husk layers intact, so a single-component model for Adlai grain is acceptable, at least for the study.

A non-conjugate diffusion-based model was used in this study wherein the heat and mass transfer inside the product are computed without affecting the flow, temperature, and water vapor concentration in the flow field of the drying air. To model the moisture content inside the product, an effective diffusivity is used, which is obtained only through experimentation. The boundary conditions at the interface require values of convective heat transfer coefficient and convective mass transfer coefficient to account for the heat and mass exchange between the product and the drying air (Sun 2019).

In the numerical solution using the Fluent solver, the steady state solution was done before conducting the transient simulation, where the drying air temperature near the kernel surface is set at the initial kernel temperature, and the moisture content of the air is in equilibrium with the kernel's (Sun 2007). Constant air velocity (1 m/s) and temperature (30°C, 45°C, and 60°C) were used at the air inlet. The drying air originated from the bottom of the domain. Zero temperature and moisture gradients were placed on the walls of the flow field. The moisture content of the drying air was not considered in the simulations due to the non-conjugate approach adopted for the study. The SST-kω model was used for turbulence modeling. An initial value for the temperature and moisture of the kernel was set. The initial moisture content (M_0) was 0.1867 MC d.b. while the kernel temperature (T_0) was set to 27°C. The initial conditions for the first stage of the solution were:

$$M(x,y,z,0) = M_0 \quad (3)$$

$$T(x,y,z,0) = T_0 \quad (4)$$

User-Defined Scalar (UDS) equation was used to simulate the moisture content within the kernel. Ansys Fluent solver uses the following UDS equation:

$$\frac{\partial \rho \phi_k}{\partial t} + \frac{\partial}{\partial x_i}\left(\rho u_i \phi_k - \Gamma_k \frac{\partial \phi_k}{\partial x_i}\right) = S_{\phi_k} \quad k=1,\ldots,N \quad (5)$$

From left to right, an unsteady term, convective term, diffusion term, and source term comprise the UDS equation as presented in Equation 5. Since it was assumed that the primary driving force for the drying of the kernel is diffusion, only the unsteady and diffusion terms were considered for the model (Chilka and Ranade 2018).

After the steady state solution, the weighted average values of the convective heat transfer coefficient (h) were calculated at the concentration profile of the air control volume next to the kernel surface. The h values were used for the heat flux at the air-kernel interface. The convective mass transfer coefficient (h_m) was calculated from its relationship with the effective diffusivity, D_e, and drying constant, k (1/s):

$$D_e = \frac{kr^2}{\pi^2} \quad (6)$$

$$k = h_m\,(A/V) \quad (7)$$

where r is the characteristic length of the grain (m), A is the surface area of the kernel (m^2), and V is the volume of the kernel (m^3). The volume and surface area of the kernel were obtained by calculating the cell volume and cell surface area of the 3D object (Adlai kernel) through Fluent, respectively.

The Neumann boundary condition was used at the air-kernel interface of the grain model. This boundary type assumes constant convective heat and mass transfer coefficients (ElGamal et al. 2014). This type of boundary condition is most commonly used due to its simplicity. The h_m values were assumed to be constant during the drying process and were used for the formulation of the mass flux equation at the interface, while the D_e values were used as inputs for the material properties of the kernel. The heat and mass flux boundary conditions at the air-kernel interface were as follows:

$$-q = h(T_s - T_\infty) \quad (8)$$

$$-\dot{m} = h_m(M_s - M_e) \quad (9)$$

In Equation 8, q is the heat flux (W/m^2), h is the convective heat transfer coefficient (W/m^2-K), T_s is the surface temperature of the kernel (K), and T_∞ is the drying air temperature (K). In Equation 9, $\dot{m}$ is the

mass flux, h_m is the convective mass transfer coefficient (m/s), M_s is the surface moisture of the grain ($kg_{water}/kg_{dry\ matter}$), and M_e is the equilibrium moisture content of the grain ($kg_{water}/kg_{dry\ matter}$).

The equations representing the boundary conditions were directly imposed on the air-kernel interface via the named expressions feature of Ansys Fluent. This has become an alternative method to the commonly used CFD technique of writing user-defined functions (UDFs).

The CFD simulations were run on an Acer Nitro AN515-55, Intel Core i7-10750H, 2.60 GHz laptop. For pressure-velocity coupling, the SIMPLE (Semi-Implicit Method for Pressure-Linked Equations) algorithm was used. For pressure, momentum, energy, turbulence, and UDS equations second order discretization scheme was used. Residuals for energy, flow, and UDS equations were set at 1×10^{-05}. Transient simulations were carried out at a time step size of 1s with 10 iterations per time step. This time step size was used in the study because there was observable modeling difficulty when using smaller time steps. For this reason, 1s was considered the minimum time step size for the best possible model accuracy given the study's parameters. The termination time of simulation was 1,265 min, 1,145 min, and 785 min for 30°C, 45°C, and 60°C drying air temperature, respectively. The modeling time went on from 16.5 h to 18 h per simulation.

The volume-weighted averages of the moisture content (UDS Scalar 0) in the kernel domain were calculated at the end of each specified number of time steps to determine the average moisture content of the kernel. These values were recorded to constitute the predicted drying performance by the CFD model.

Validation of the CFD Models

To validate the acceptability of the simulated drying curves resulting from CFD modeling, specific statistical parameters were used as basis. These parameters determine the model accuracy and goodness-of-fit with respect to the experimental data from the thin-layer drying experiment. These statistical parameters were the coefficient of determination (R^2), the standard error (S), and the percent mean deviation modulus (P%). The latter must be less than 10% for the model to be acceptable (Mohapatra and Rao 2005).

The R^2 and S values were calculated through the built-in data analysis tools in Microsoft Excel 2016 while the P% values were calculated using the equation:

$$P\% = \frac{100}{n} \Sigma \frac{abs(M_i - M_{pre})}{M_i} \quad (10)$$

where M_i is the moisture content from the experiments, M_{pre} is the predicted moisture content from the CFD simulations, and n is the number of observations. It should be noted that the predicted and experimental moisture values compared were of the same time step.

RESULTS

Thermophysical Properties of Adlai

The thermophysical properties of Adlai used in the CFD simulations were estimated using mathematical models involving the food constituents of the product. The estimated values of thermal conductivity, specific heat, and true density of Adlai are presented in Table 3. For drying air temperature range of 30°C to 60°C, the thermal conductivity of Adlai ranged from 0.1491 to 0.1628 W/m^2-K, the specific heat ranged from 1,986 to 2,024 J/kg-K, and the true density ranged from 885 to 892 kg/m^3.

Table 3. Estimated thermophysical properties, effective diffusivity and convective mass transfer coefficients of Adlai grain at different drying air temperatures.

Property	Drying Air Temperature (°C)		
	30	**45**	**60**
Thermal conductivity (W/m-K)	0.1491	0.1563	0.1628
Specific heat (J/kg-K)	1986	2006	2024
True density (kg/m^3)	892	889	885
Effective Diffusivity, D_e (m^2/s)	2.772×10^{-12}	4.678×10^{-12}	7.277×10^{-12}
Convective mass transfer coefficient, h_m (m/s)	2.701×10^{-08}	4.558×10^{-08}	7.090×10^{-08}

Thin-layer Drying of Adlai

A single layer of Adlai grains was subjected to forced heated air drying using 30°C, 45°C, and 60°C at around 10% to 80% RH. The initial moisture content of the sample grains was determined to be 0.1867 MC d.b. The moisture content at specified intervals during drying was measured and recorded manually. The moisture of the grains was expressed as moisture ratio (MR) and was plotted against the drying time to generate the drying curve at different drying air temperatures. Figure 4 presents the drying curves from the thin-layer drying experiments.

Since there are no EMC values for Adlai grain available in literature, the final moisture contents at the end of the thin-layer drying experiments were adopted as approximate EMC values. The EMC values for drying air temperatures of 30°C, 45°C, and 60°C were around 13%, 11%, and 9% MC d.b., respectively.

The average drying time for the grains to reach equilibrium with the drying air was 1,265 min (21 h), 1,145 min (19 h), and 785 min (13 h) for drying air temperatures of 30°C, 45°C, and 60°C, respectively at 10% to 80%. RH.

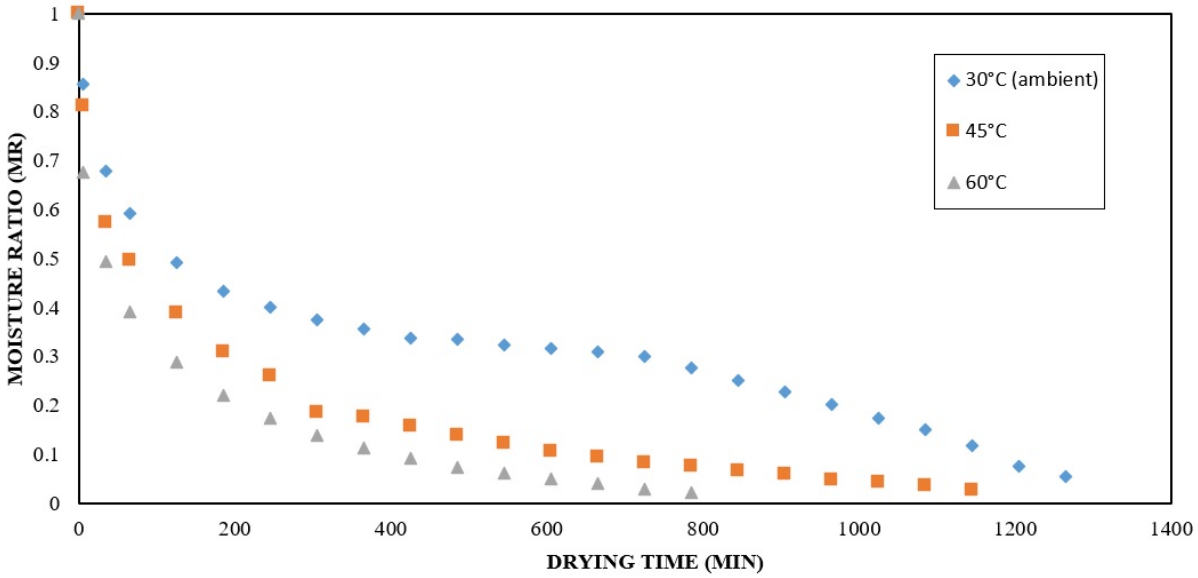

Figure 4. Experimental drying curves of Adlai grain at different drying air temperatures.

Table 4 summarizes the model constants and the average drying rates for each drying air temperature. At the drying air temperature range of 30°C to 60°C, the model constants *A* and *k* were observed to be 0.7386 to 0.8097 and 0.002 to 0.007 per min, respectively. For the same range, the average dying rate was between 0.2479 and 0.6969 % MC d.b. per h of drying.

Table 4. Simplified diffusion model constants and average drying rate during thin-layer drying of Adlai.

Drying Air Temperature (ºC)	MR = A·exp(-kt)		R^2	Average Drying Rate (% MC d.b./h)
	A	k (1/min)		
30	0.7386	0.002	0.8843	0.2479
45	0.8097	0.004	0.9451	0.3715
60	0.7878	0.007	0.9260	0.6969

The effective diffusivity (D_e) of moisture in the Adlai grain for each drying air temperature was calculated using Equation 6. The D_e values were calculated by plotting *lnMR* against drying time. The average values of the effective diffusivity are presented in Table 3. In the drying air temperature range of 30°C to 60°C, the effective diffusivity value of Adlai grain moisture ranged from 2.772×10^{-12} to 7.277×10^{-12} m^2/s.

Temperature has a more significant effect on the drying process of grains compared to the initial moisture content. The effect of temperature on the effective diffusivity was expressed through an exponential model. The values of lnD_e were plotted against the absolute drying air temperature. The plot is presented in Figure 5. The exponential model was formulated as follows:

$$D_e = 36.35exp(0.0322T_a) \quad (11)$$

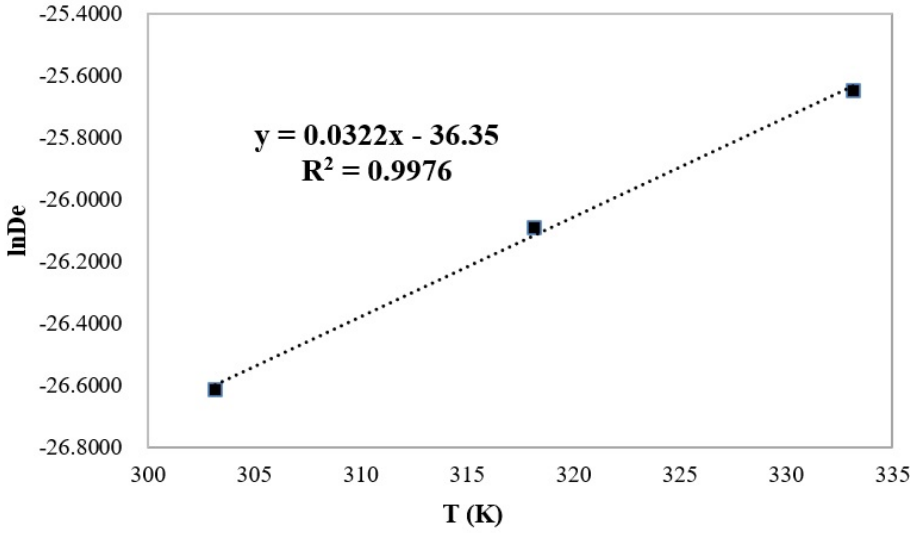

Figure 5. Plot of lnD_e vs drying air temperature (K) used in convective drying of Adlai grain.

The value for the diffusivity at infinite high temperature, D_o, was found to be 36.35, while the value of constant *c* was found to be 0.0322. The slope of the curve gives the constant *c* while the intercept gives the D_o.

The average convective mass transfer coefficient (h_m) values used to formulate the mass flux equation at the air-kernel interface of the CFD model were derived using Equation 7. The h_m values used in the study are presented in Table 3. The h_m values for Adlai kernel varied from 2.701×10^{-08} to 7.090×10^{-08} m/s for 30°C to 60°C drying air temperature. The values presented were necessary inputs for the mass flux equation at the air-kernel interface of the CFD simulations.

Computational Fluid Dynamics (CFD) Drying Simulation of Single Adlai Kernel

The average moisture content at each time interval was calculated by determining the volume-weighted average of the UDS Scalar 0 (moisture content) in the kernel domain. Figures 6-8 show the simulated moisture values from the CFD simulation and the experimental moisture values at different drying air temperatures. The drying performance of Adlai was described by the drying curves obtained by simulating the heat and moisture transfer within the Adlai grain at different drying air temperatures.

The temperature and moisture profiles within the Adlai kernel during drying can also be calculated and shown using the post-processing unit of the Fluent solver. Tables 5 and 6 show these profiles. Both the average temperature and moisture content of the kernel were determined by calculating the volume weighted average of static temperature and UDS Scalar 0 (moisture content), respectively.

Validation of the CFD Models

The experimental drying performance of Adlai grain was compared with the predicted drying performance generated by the CFD simulations. The accuracy of the fit was explained through the coefficient of determination (R^2) and the standard error (S). The percent mean deviation modulus (P%) was used to define model accuracy. These values are presented in Table 7. At the drying air temperature range of 30°C to 60°C, the R^2 values ranged from 0.94 to 0.98, S values ranged from 0.0018 to 0.0066, and P% values ranged from 6.5% to 8.68%, respectively.

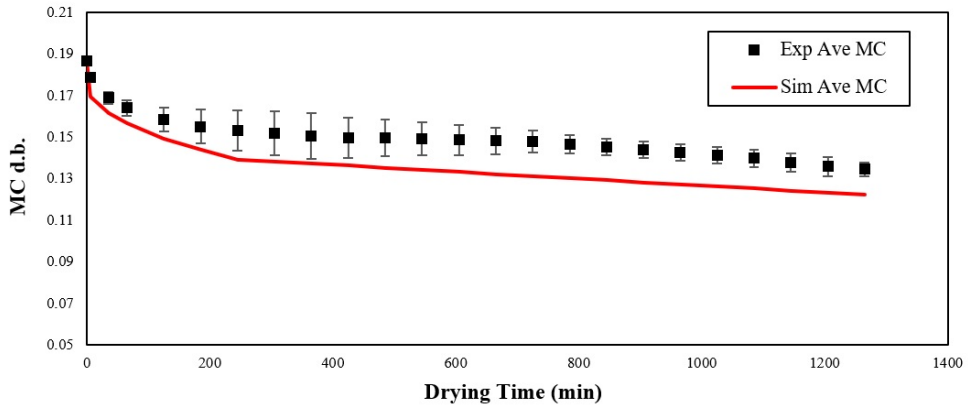

Figure 6. Experimental and predicted drying curves of Adlai at 30°C drying air temperature.

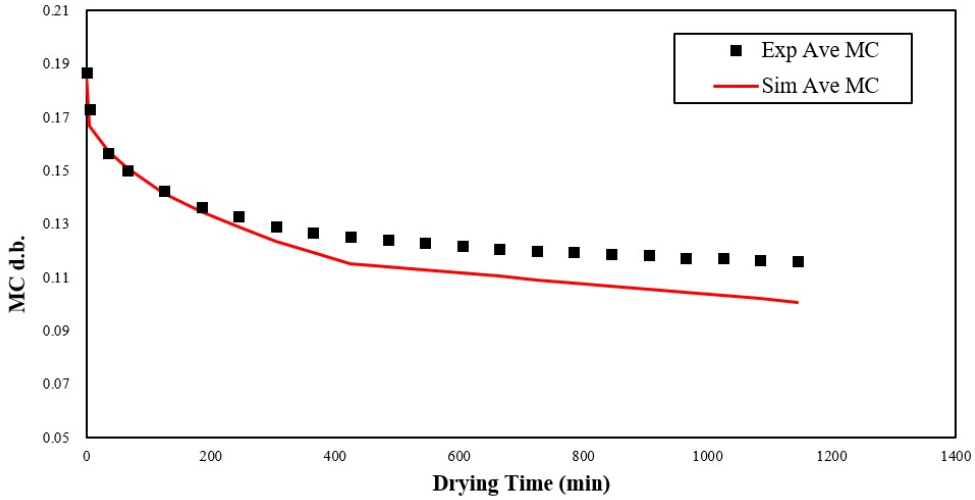

Figure 7. Experimental and predicted drying curves of Adlai at 45°C drying air temperature.

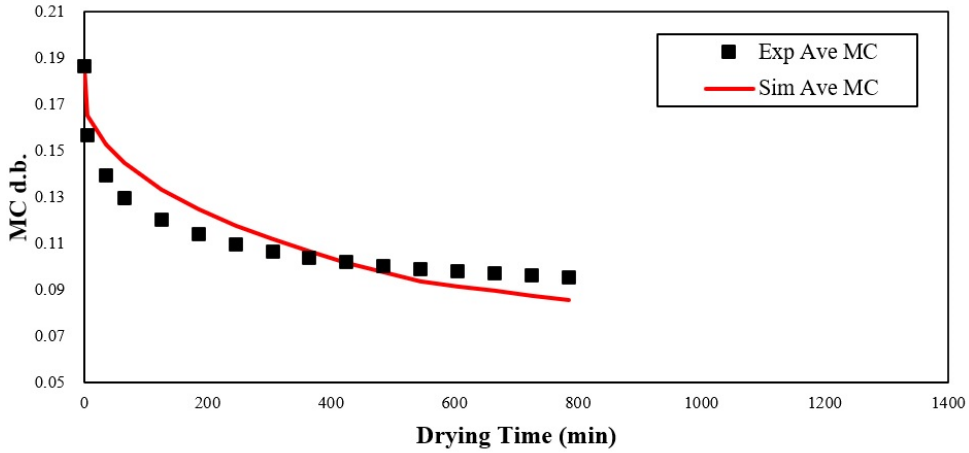

Figure 8. Experimental and predicted drying curves of Adlai at 60°C drying air temperature.

Table 5. Moisture profile of Adlai kernel at 60°C drying air temperature.

Legend	Moisture Profile			
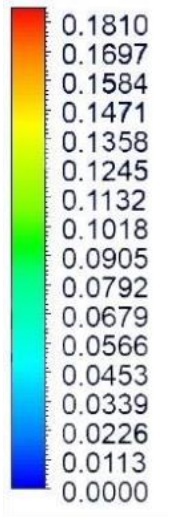	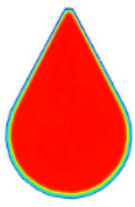	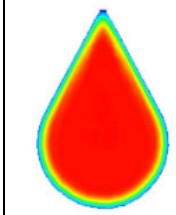	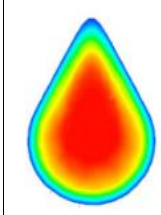	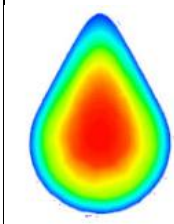
	Moisture Content (d.b.) and Drying Time (min)			
	0.1653 t = 5 min	0.1148 t = 65 min	0.1119 t = 305 min	0.0917 t = 605 min

Table 6. Temperature field and profile of Adlai kernel at 60°C (333.15 K) drying air temperature.

Legend	Temperature Profile		
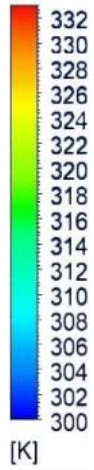	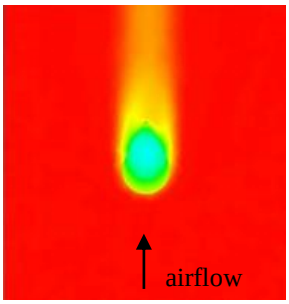	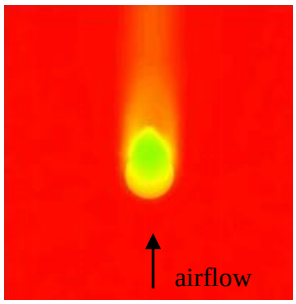	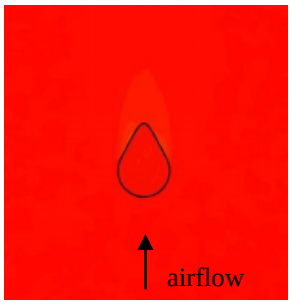
	Temperature (K) and Drying Time (s)		
	T = 316 K t = 30 s	T = 324 K t = 60 s	T = 332 K t = 150 s

Table 7. Statistical parameters indicating model accuracy.

Drying Air Temperature (°C)	R^2	S	P%
30	0.98	0.0018	8.68
45	0.98	0.0027	6.94
60	0.94	0.0066	6.50

DISCUSSION

Thermophysical Properties of Adlai

Standard experimental methods for calculating selected thermophysical properties of Adlai were not performed since the study was conducted during the COVID-19 pandemic when there were restrictions to travel, work, and other activities. Estimation of the values through mathematical modeling was the available alternative.

Mathematical modeling of the thermophysical properties of food was used in the study to calculate the values of thermal conductivity, specific heat, and true density of Adlai, which were necessary inputs for the CFD simulations. These values were used in the material properties panel for the solid cell zone of the CFD models, representing the Adlai kernel. It was observed that the estimated thermal conductivity and specific heat of the Adlai grain increased as the assumed kernel temperature increased, while the opposite was observed for the estimation of true density.

Thin-layer Drying of Adlai

According to the drying curves presented in Figure 3, it was observed that the lower the drying air temperature used, the longer the drying time to reach equilibrium. Higher drying air temperature is usually accompanied by a lower RH, allowing for higher moisture transfer between the kernel and the surrounding air. As shown in Table 4 higher average drying rates (% MC d.b. per h) are achieved at higher air temperatures and lower RH. The average drying rate shows the amount of percent moisture reduction during drying. However, it does not show the high initial moisture removal rate at the beginning of drying since it is averaged over the entire drying time.

The accuracy of the fit of the simplified diffusion model with the experimental drying curves of Adlai grain improved as the drying air temperature increased. This observation was based on the increase in the R^2 value between the models and the experimental drying curves. At higher drying temperatures, the R^2 values were over 0.9 which indicate better fit of the model values with the experimental moisture values from the thin-layer drying experiment.

It was observed that the effective diffusivity of moisture within the grain increased proportionally with the drying air temperature. This was also observed by Jha and Tripathy (2021) in their simulation of heat and mass transfer of solar drying of paddy. For cereal grains, the effective diffusivity found in literature falls within the range of 10^{-13} to 10^{-08} m^2/s. Based on this condition, the estimated D_e values of Adlai fall within the accepted range. The effective diffusivity of the Adlai grain's moisture is associated with higher drying rates when higher drying air temperatures are used. This is because more moisture diffuses and leaves the kernel when it is exposed to higher air temperatures at lower RH. The moisture diffusion within the kernel was less affected by the internal resistances at higher drying air temperatures.

The convective mass transfer coefficient (h_m) describes the rate of moisture transfer from the surface of the kernel to the drying air, thus affecting the moisture reduction rate within the kernel's volume. It was observed that the higher the temperature of the drying air, the higher the h_m value. This was also similar with the data of Nguyen et al. (2019) in the study of experimental and numerical investigation of transport phenomena and kinetics of convective shrimp drying. The convective mass transfer coefficient values calculated in this study indicate that the moisture removal at the kernel's surface is more significant and occurs more rapidly at higher drying air temperatures. This is because at higher drying air temperatures, the relative humidity is usually lower, allowing for greater moisture transfer from the grain to the surrounding air.

Computational Fluid Dynamics (CFD) Drying Simulation of Single Adlai Kernel

Visually, the simulated drying performance of the Adlai grain via CFD modeling fitted closely with the experimental drying performance when plotted together. Agreement between the simulated and the experimental drying curves was better during the initial hours of drying and gradually deteriorated in the latter stages, which was also reported by Chandramohan (2016) in his coupled CFD model for convective drying of a moist object. The numerical models for 30°C, 45°C, and 60°C have the same initial moisture content of 0.1867 and duration of drying time as with the thin-layer drying experiments. However, the final moisture contents were different for simulated and experimental drying curves. The final moisture contents from simulated and experimental drying using 30°C-60°C drying air temperature were 0.1221 to 0.0857 MC d.b. and 0.1344 to 0.0955 MC d.b., respectively. From the data presented, it is clear that the numerical moisture values underestimated the experimental moisture values because the simulations approached the EMC of Adlai at a much faster drying time than the thin-layer drying experiments. For drying temperatures of 30°C, 45°C, and 60°C, the simulation approached Adlai's EMC at around 785 min, 665 min, and 605 min, respectively. The reason behind this could be the constant average values of effective diffusivity and convective mass transfer coefficients. Variable effective diffusivity and convective mass transfer coefficient values would get smaller as the drying process proceeds such that at later stages in drying, the moisture reduction in the model would not be as significant as using constant

values. This would make the agreement between the simulated and experimental moisture values better. Furthermore, the study did not consider physical changes in the grain, which can cause resistance to moisture diffusion and evaporation during the drying phenomenon. Changes such as shrinkage, cracking, and case hardening were not investigated while conducting the thin-layer drying experiments at different drying air temperatures. Nevertheless, these physical changes in the grain have been found out to have an effect on the rate of moisture removal during drying.

Aside from the drying performance over time, the moisture and temperature profiles during the CFD simulations of convective drying of Adlai grain can be visualized through Ansys Fluent. The apex of the Adlai grain model was positioned away from the drying air inlet of the simulation such that the drying air hit the bottom of the grain first. This was the geometric presentation chosen for the study since different orientations of the kernel to airflow direction did not show any effect on the average moisture content of the grain with similar drying conditions. This was also reported by ElGamal et al. (2014) for the convective drying simulation of a single rice kernel. It was assumed that moisture transfer occurs at the kernel's surface, creating areas of varying moisture content within the kernel in the process, as shown in Table 5. It was observed that during the simulation of convective drying of a single kernel of Adlai, moisture reduction occurs much faster near the kernel's surface than the core. As shown in Table 5, as the drying time increased, the moisture content at the center of the grain decreased as well. The moisture diffused from the center of the grain to the surface, where moisture vaporization took place, leaving the regions near the surface with low moisture content. This was also observed in the numerical study of heat and mass transfer of peanut drying (Chen et al. 2023). Over time, the moisture at the core of the grain reduced further, as indicated by the recession of high moisture color bands in the model's geometric profile. The reduction of moisture content in the kernel affected the overall average moisture content of the entire kernel. This phenomenon eventually gave the final moisture content of the grain at the termination of the drying simulation. It was observed that high moisture concentration at the kernel's core would also give a high average kernel moisture value.

Heat transfer during the drying simulation occurred significantly faster than the mass transfer. This was also parallel in the works of Chilka and Ranade (2018) and Nguyen et al. (2019) in drying almond kernel and shrimp, respectively. It took only a short period of time for the kernel temperature to achieve thermal equilibrium with the drying air temperature as shown in Table 6. Over time, the color gradient in the kernel changed as the temperature increased and became approximately equal to the drying air temperature. At 150 s and further, the kernel temperature is in equilibrium with the drying air temperature. Colored streaks formed around the kernel, indicating its solid-fluid interaction with the moving drying air.

The heat transfer mechanism in Fluent is dependent on the thermophysical properties given to the solid (kernel) cell zone and the fluid (drying air) cell zone. These separate cell zones interact at the air-kernel interface, which has been treated as a coupled boundary between the solid and fluid cell zones.

Moisture and temperature profiles within the kernel via CFD modeling offer essential insights regarding its drying behavior. Moisture variation within the kernel allows the management of potential hygroscopically induced fissuring or cracking. Thus, the decision to incorporate tempering in the drying process could be made if necessary. Also, analyzing the moisture movement and variation within the kernel would help food technologists understand the diffusion mechanism of moisture from the endosperm to the husk to complete the moisture removal process at the surface. However, in the case of Adlai, this would entail further investigations of the properties of its endosperm, bran layer, and husk. When it comes to the temperature profile of grain, understanding the temperature variation within the kernel helps manage grain drying while minimizing the effects of thermal stress that may be caused by rapid drying. All of these are important to the food technologist since the drying rate of grain greatly affects the final quality of the kernels (Bonazzi et al. 1997).

Validation of the CFD Models

As shown in Table 7, the simulation for 60°C drying air temperature was the lowest in terms of R^2 value since it is the only one lower than 0.98. However, both models for 30°C and 45°C drying air temperature have higher P% values, which is indicative of higher deviation from the experimental data. In general, all the predicted models from the CFD simulations were acceptable due to their high R^2 values, low S values, and P% values of less than 10%. This means that CFD modeling is an acceptable technique for predicting the drying performance of Adlai grain under several convective drying temperatures. This method could be used apart from full-scale experimentation, which is deemed laborious, expensive, and time-consuming. CFD could be used to explore the behavior of Adlai under several other drying conditions.

FUNDING

This study would not have been possible without the support of the Department of Science and Technology – Engineering Research and Development for Technology (DOST-ERDT).

ETHICAL CONSIDERATIONS

No human or animals were involved nor harmed in the conduct of this study.

DECLARATION OF COMPETING INTEREST

The authors of this study declare that there are no competing interests of any kind with other authors.

ACKNOWLEDGMENTS

The authors would like to thank DOST-ERDT for being the primary funding agency of this research endeavor. Immense gratitude is extended by the corresponding author to those who contributed to the success of this study, as well as to his family, his friends, and the faculty members and staff of the University of the Philippines Los Baños – College of Engineering and Agro-Industrial Technology (UPLB-CEAT). The comments and suggestions of the two anonymous reviews helped improve the contents of this research work.

REFERENCES

Andoy CN, Enot IR, Mabaza AD and Quillo IC. 2019. Utilization of Job's tear (*Coix Lacryma-Joba L.*) flour as composite for all purpose flour in saltine crackers. American Journal of Biomedical and Life Sciences, 7(3): 52. https://doi.org/10.11648/j.ajbls.20190703.12

Aradilla, AR. 2018. Phenology, growth and yield performance of adlay (*Coix lacryma-jobi* L.) grown in adverse climatic conditions. International Journal of Research & Review, 5(3): 16-24.

Bonazzi C, Peuty MA and Themelin, A. 1997. Influence of drying conditions on the processing quality of rough rice. Drying Technology, 15(3-4): 1141-1157. https://doi.org/10.1080/07373939708917283

Carson JK, Wang J, North MF and Cleland DJ. 2016. Effective thermal conductivity prediction of foods using composition and temperature data. Journal of Food Engineering, 175: 65–73. https://doi.org/10.1016/j.jfoodeng.2015.12.006

Cengel YA and Cimbala JM. 2014. Property Tables and Charts. Fluid Mechanics: Fundamentals and Applications Third Edition. McGraw-Hill, New York, USA, 948 pp.

Chandramohan VP. 2016. Experimental analysis and simultaneous heat and moisture transfer with coupled CFD model for convective drying of moist object. International Journal for Computational Methods in Engineering Science and Mechanics, 17(1): 59–71. https://doi.org/10.1080/15502287.2016.1147506

Chen P, Chen N, Zhu W, Wang D, Jiang M, Qu C and Li Y. 2023. A heat and mass transfer model of peanut convective drying based on a two-component structure. Foods, 12: 1823. https://doi.org/10.3390/foods12091823

Chilka AG and Ranade VV. 2018. Drying of almonds I: single particle. Indian Chemical Engineer, 60(3): 232–254. https://doi.org/10.1080/00194506.2017.1333464

ElGamal R, Ronsse F, Radwan SM and Pieters JG. 2014. Coupling CFD and diffusion models for analyzing the convective drying behavior of a single rice kernel. Drying Technology, 32(3): 311–320. https://doi.org/10.1080/07373937.2013.829088

Ibarz A and Barbosa-Canovas GV. 2014. Thermal Properties of Foods. Introduction to Food Process Engineering First Edition. CRC Press, Taylor & Francis Group, Boca Raton, Florida, USA, pp. 198-207.

Jha A and Tripathy PP. 2021. Optimization of process parameters and numerical modeling of heat and mass transfer during simulated solar drying of paddy. Computers and Electronics in Agriculture, 187: 106215. https://doi.org/10.1016/j.compag.2021.106215

Keeratibunharn N and Krasaekoopt W. 2013. Development of Job's tears yogurt. Assumption University Journal of Technology, 16(3): 133–139.

Khongjeamsiri W, Wangcharoen W, Pimpilai S and Daengprok W. 2007. Preference direction study of Job's tears ice cream. Maejo International Journal of Science and Technology, 01(2): 137-144.

Kim HS, Kim OW, Kim H, Lee HJ and Han JW. 2016. Thin layer drying model of sorghum. Journal of Biosystems Engineering, 41(4): 357–364. https://doi.org/10.5307/jbe.2016.41.4.357

Kumar C, Karim A, Joardder MUH and Miller GJ. 2012. Modeling heat and mass transfer process during convection drying of fruit. In Gu, Y T & Saha, S (Eds.) Proceedings of the 4th International Conference on Computational Methods. Queensland University of Technology, Australia, pp. 1-8.

Mohapatra D and Rao PS. 2005. A thin layer drying model of parboiled wheat. Journal of Food Engineering, 66(4): 513–518. https://doi.org/10.1016/j.jfoodeng.2004.04.023

Nguyen MP, Ngo TT and Le TD. 2019. Experimental and numerical investigation of transport phenomena and kinetics for convective shrimp drying. Case Studies in Thermal Engineering. 14: 100465. https://doi.org/10.1016/j.csite.2019.100465

Peleg M, Normand MD and Corradini MG. 2012. The Arrhenius equation revisited. Critical Reviews in Food Science and Nutrition, 52(9): 830–851. https://doi.org/10.1080/10408398.2012.667460

Peñaflor LM, Elepaño AR and Peralta EK. 2014. Rice-like grains from broken rice *(Oryza sativa L.)* and adlai (Coix lacryma-jobi L.). Asian Journal of Agriculture and Food Science, 02(04): 2321–1571.

Prakash B and Pan Z. 2011. Modeling Moisture Movement in Rice. Advanced Topics in Mass Transfer. InTech, Rijeka, Croatia, pp. 283-304.

Sun DW. 2007. CFD Modeling of Simultaneous Heat and Mass Transfer in Beef Chilling. Computational Fluid Dynamics in Food Processing. CRC Press, Taylor & Francis Group, Boca Raton, Florida, USA, pp. 195-221.

Sun DW. 2019. Non-Conjugated Drying Models. Computational Fluid Dynamics in Food Processing Second Edition. CRC Press, Taylor & Francis Group, Boca Raton, Florida, USA, pp. 342-344.

The Engineering ToolBox. 2018. Air - Diffusion Coefficients of Gases in Excess of Air. https://www.engineeringtoolbox.com Accessed on 13 January 2021.

ROLE OF AUTHORS: *AMA – main author, concept, numerical modeling, data gathering, data analysis, manuscript writing; ARE – thesis adviser, concept, consultations, revising of manuscript; KFY – consultations, revising of manuscript; DCS – consultations, revising of manuscript.*